Trees (2021) 35:1233–1245
https://doi.org/10.1007/s00468-021-02111-0

ORIGINAL ARTICLE

Poplar root anatomy after exposure to elevated O_3 in combination with nitrogen and phosphorus

Tanja Mrak[1] · Natalija Dovč[1] · Jožica Gričar[1] · Yasutomo Hoshika[2] · Elena Paoletti[2] · Hojka Kraigher[1]

Received: 13 July 2020 / Accepted: 27 February 2021 / Published online: 23 March 2021

Abstract

Key message **Elevated O_3, particularly in interaction with N and/or P levels, induced tissue- and cell type-specific changes in the anatomical structure of poplar roots.**

Abstract Ozone (O_3) sensitive poplar clone *Populus maximowiczii* Henry × *berolinensis* Dippel was subjected to two levels of O_3 (ambient and 2 × ambient) in combination with two levels of nitrogen (N) (0 and 80 kg ha^{-1}) and three levels of phosphorus (P) (0, 40 and 80 kg ha^{-1}) in an open-air pot experiment. Effects of O_3 in combination with N and P on anatomical structure of xylem, bark and primary tissues and consequences for theoretical hydraulic properties were investigated after one growing season in 2-mm roots under the microscope. Effect of O_3 as single factor was observed as increased primary xylem area and number of protoxylem poles, increased secondary xylem area and accumulated potential hydraulic conductivity. Vessel density, but not vessel size was negatively affected by O_3. Stronger correlation between tangential vessel diameter and vessel density was encountered under ambient O_3, indicating a slight dysregulation of vessel formation under elevated O_3. Increasing P resulted in increased number of protoxylem poles, while N mostly acted in interaction with O_3 or P. There was a strong interaction between $O_3 \times N \times P$ on vessel grouping index and mean vessel group size. At elevated O_3, effects of both nutrients on vessel grouping and mean vessel group size were repressed. Under ambient O_3, application of N resulted in increased fibre cell thickness, which was not the case under elevated O_3, indicating carbon-saving mechanisms.

Keywords Root tissues · Primary xylem · Secondary xylem · Vessel grouping index · Theoretical conductivity · Fibre cell wall

Introduction

Poplars (*Populus* spp.) are widely distributed in their native range within the northern hemisphere, while plantations are established on both hemispheres. As a fast growing tree species, they are an increasingly important renewable resource of biomass in a growing bioeconomy (Lewandowski et al. 2019). Due to their fast growth rate, they have high nutrient requirements and a high sensitivity to ozone (O_3). Poplars often face nutrient limitations in relation to their high productivity, limited nutrient availability in native soil, and nutrient imbalances due to this. Nitrogen (N) has been recognised as the most limiting nutrient for poplar growth, but within some sites phosphorus (P) might be limiting too (Isebrands and Richardson 2014). Tropospheric ozone (O_3) is a phytotoxic air pollutant that affects plant metabolism through the generation of free radicals (Monks et al. 2015). Globally, tropospheric ozone concentrations have increased by 30% since the pre-industrial era (Young et al. 2013). In some parts of the world, emissions of O_3 precursors are still growing, thereby affecting ozone concentrations on a global scale (Verstraeten et al. 2015). Elevated O_3 further affects trees through reduced Rubisco and chlorophyll content, leaf area, transpiration rates, height and tree diameter, root to shoot ratio and the total tree biomass (Wittig et al. 2009).

Several studies have shown that O_3, N and P as single factors can affect the tissue structure of poplars and other broadleaved tree species (Table S1), while the interactive effects

Communicated by Grams.

✉ Tanja Mrak
tanja.mrak@gozdis.si

[1] Slovenian Forestry Institute, Večna pot 2, 1000 Ljubljana, Slovenia

[2] Institute of Research on Terrestrial Ecosystems (IRET), National Research Council of Italy (CNR), Via Madonna del Piano 10, 50019 Sesto Fiorentino, FI, Italy

of O_3 and these two nutrients are less well investigated. Most past studies have been performed on the secondary xylem of the stem due to the economic importance of wood, mainly focusing on vessel size and fibre characteristics (Table S1). Anatomical changes in the secondary xylem are extremely important for the survival of trees under stress. Changes in vessel diameters may have a pronounced effect on the efficiency of water transport on one hand, and on the hydraulic safety on the other. Vessel size is a trade-off between water transportation efficiency and vulnerability to cavitation. Even a small increase in vessel diameter increases water conductivity immensely (Hagen-Poiseuille equation), but the side effect is a higher risk of embolism due to drought or freezing (Tyree and Zimmermann 2002). N and P may affect vessel arrangement (Spannl et al. 2016) with possible implications for vulnerability to cavitation (von Arx et al. 2013 and references therein, Schuldt et al. 2016), while no data are available for O_3. There are some indications that tissues other than the secondary xylem might also be affected by O_3 and N, but the effect of P is to our knowledge, not known (Table S1). Previous studies focusing mainly on tree biomass and physiology (e.g.Pell et al. 1995; Schmutz et al. 1995; Maurer and Matyssek 1997; Utriainen and Holopainen 2001; Watanabe et al. 2012) have emphasised the ability of N to modify O_3 response in plants.

Roots are an integral tree component and are crucial for the absorption of water and nutrients along with their transport to the aboveground parts of the tree, the storage of non-structural carbohydrates and N, and for tree anchoring. Despite their importance to plant functioning, roots and specifically root anatomical structure are rarely considered in stress-effect studies. While tree roots come in direct contact with nutrients the effect of elevated O_3 on roots is indirect, occurring through reduced carbon supply to belowground parts (Andersen 2003) and through plant hormonal shifts (Kraigher et al. 2008). Although the effect of elevated O_3 on roots is indirect, they may occur before any change is observed aboveground (Andersen 2003). The greater effect of elevated O_3 in the lower stem when compared to middle stem was explained by the greater distance of the lower stem from leaves as carbon source which may be true for roots (Richet et al. 2011).

In our study, the effects of elevated O_3 in combination with different levels of N and P fertilisation on the anatomical structure of xylem, bark and primary tissues and consequences for theoretical hydraulic properties were investigated in roots of an O_3-sensitive poplar clone. We hypothesized that a greater nutrient supply will result in wider vessels, and therefore, a higher potential xylem-specific conductivity of roots to be able to support the greater biomass. This was previously reported for the plants from the same experiment due to addition of N (Zhang et al. 2018). We expected that the negative effects of elevated O_3, such as smaller tissue widths and smaller vessel sizes in root tissues of the secondary xylem and bark and secondary xylem cells, will be more pronounced at a high P and N nutrient supply. We hypothesised that different levels of the investigated factors would affect the association between vessel density and vessel size. Although vessel density and vessel tangential diameter are supposed to be highly correlated (Schume et al. 2004, Savage et al. 2010), our previous study on oaks (Mrak et al. 2019) showed that vessel density proved to be more sensitive indicator of O_3 concentration alterations than vessel size, indicating dysregulative effects of elevated O_3 on this relationship.

Methods

Propagation, planting and ozone/nutrient treatments

The O_3-sensitive poplar clone, i.e. *Populus maximowiczii* Henry × *berolinensis* Dippel (Oxford poplar clone) (Marzuoli et al. 2009, Hoshika et al. 2018) was selected for the experiment. Cuttings obtained in December 2015 were potted in February 2016 and kept in a greenhouse. In March 2016, they were moved outside to the experimental garden of CNR at Sesto Fiorentino, Italy (43°48′49″ N, 11°12′01″ E, 55 m a.s.l.) where the O_3 free-air controlled exposure (FACE) facility is located (Paoletti et al. 2017). In April 2016, they were planted into 10-L pots filled with a substrate mixture of peat:sand:local soil in 1:1:1 ratio. The local soil had a sandy-loam texture and a slightly acidic pH. At the time of planting the initial average height of plants was 15.4 cm. The substrate was fertilised with two levels of N, 0 and 80 kg ha^{-1}, combined with three levels of P, 0, 40 and 80 kg ha^{-1} (Zhang et al. 2018; Mrak et al. 2020), resulting in six treatment combinations N0P0, N80P0, N0P40, N80P40, N0P80 and N80P80. 40 kg ha^{-1} corresponded to 196.3 mg per plant and 80 kg ha^{-1} to 392.5 mg per plant for the experimental time period May 1st 2016 to October 1st 2016. Levels of N were selected to simulate the minimum and maximum levels of background N deposition worldwide (0 and 80 kg N ha^{-1}, Fenn et al. 2003; Peng et al. 2017). While there is not a significant amount of atmospheric P deposition, poplar plantations are usually established in various soil nutritional conditions (low-fertilised volcanic ash soils, Hoosbeek et al. 2004; high-fertilised agricultural field soils, Arevalo et al. 2011). Levels of P were, therefore, determined to simulate a realistic P concentration in soils. Levels of N and P in the soil ranged between 1.71 and 2.84 g kg^{-1} for N and between 0.49 and 1.12 g kg^{-1} for P in different treatment combinations at the end of experiment (see Zhang et al. 2018) and agreed with realistic N and P concentrations

in soils (N: 0.2–5.0 g kg^{-1}, Bowen 1979; P: 0.5–1.3 g kg^{-1}, Stevenson and Cole 1999).

Fertilisation with P was performed with 0, 0.5 and 1.0 mM KH_2PO_4 solution according to Lewis and Strain (1996) and N was supplied as 0 and 5 mM solution NH_4NO_3 according to Thomas et al. (1994).

The substrate was fertilised with 200 mL solution of NH_4NO_3 or KH_2PO_4 with the above-stated concentrations twice a week throughout the experiment. To keep an equal amount of K among all treatments, KCl was added to the substrate that did not receive KH_2PO_4 at the same time (Tissue and Lewis 2010; Mao et al. 2014). In addition to N and P, soil concentrations of C, K, Fe, Ca and Mg and pH were measured at the end of the experiment and were reported by Zhang et al. (2018).

Poplar plants were subjected to two levels of O_3: ambient (AA—referred as control, 35.0 ppb as daily average O_3 concentration) and 2.0 × ambient (2.0 × AA—referred as elevated, 66.7 ppb as daily average O_3 concentration) at an O_3 FACE facility (Paoletti et al. 2017) for the period between May 1st, 2016 and October 1st, 2016. Each of 12 treatment combinations [(two levels of O_3) × (two levels of N) × (three levels of P)] was replicated in three plots of the FACE facility, and each replicate contained three poplar plants. Treatment combinations and the final height of the plants are given in the Supplementary material (Table S2). For anatomical analyses, one of three poplars per replicated plot was selected, i.e. three poplars per treatment, while the remaining plants were used for other investigations. Due to use of sufficiently large pots, roots did not reach the bottom of the pot at the end of experiment, neither were they intertwined.

Root sampling and microscopy

From each seedling, three roots with 2-mm diameter were randomly selected. From each selected root, one 5-mm-long section was cut with blade and fixed in formaldehyde-ethanol-acetic acid (FAA). Samples were dehydrated in a graded series of ethanol, embedded in paraffin and cut with a Leica RM 2245 rotary microtome (Leica Microsystems, Wetzlar, Germany) to obtain cross-sections of 10 µm in thickness, which were mounted onto object slides and stained with a safranine–astra blue water mixture and finally embedded in Euparal, for details see Mrak and Gričar (2016).

Sections were photographed in bright field using Zeiss AxioImagerZ2 microscope (Carl Zeiss Microscopy GmbH, Jena, Germany) at 100 × magnification. ZEN 2012 software (Carl Zeiss Microscopy GmbH, Jena, Germany) was used to compose panorama photos.

On the photographed sections, the shape of the primary xylem (i.e. number of protoxylem poles) was recorded. The presence of intraannual density fluctuations (IADFs) in the secondary xylem, defined as areas with abrupt change in wood density inside the growth ring (De Micco et al. 2016) was recorded as well. IADFs reflect variations in climatic conditions during the growing season (De Micco et al. 2016). In the secondary xylem, vessel number, vessel size

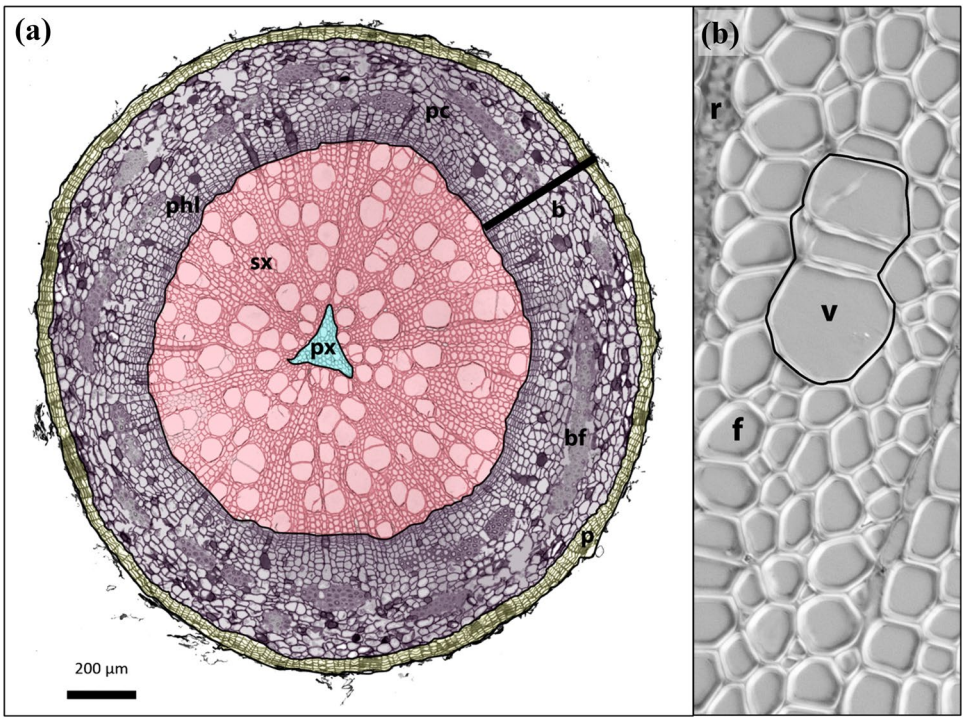

Fig. 1 **a** Cross-section of 2-mm root of poplar cutting after one growing season. *Px* primary xylem, *sx* secondary xylem, *phl* phloem, *pc* pericycle, *bf* bark fibres, *b* bark, *p* periderm. Bark includes phloem, pericycle, bark fibres and periderm. **b** Close-up view of secondary xylem using differential interference technique. *V* vessel, *r* xylem ray, *f* fibre of secondary xylem. Encircled vessels form vessel group

(tangential vessel diameter, vessel area) and vessel arrangement were measured using ROXAS software (von Arx and Dietz 2005; von Arx et al. 2013; von Arx and Carrer 2014) which carried out automatic calculations of vessel density, cumulative area of vessels, percentage of conductive area within the secondary xylem, accumulated potential hydraulic conductivity (K_h; *K* as approximated by Poiseuille's law and adjusted to elliptical tubes, Eq. 1, Tyree and Zimermann 2002) and xylem-specific potential hydraulic conductivity (K_h/xylem area):

$$K_{\text{ellipse}} = \frac{\pi}{64\eta}\frac{a^3b^3}{a^2+b^2}, \quad (1)$$

where *a* and *b* are the major and minor axes of the ellipse and η is the dynamic viscosity of the liquid (Tyree and Zimermann 2002).

Tissue parameters (mean width of periderm, bark, secondary xylem, and area of the secondary and primary xylem) were measured using ZEN 2012 software (Fig. 1a). From these measurements, tissue width ratios (periderm to bark, bark to secondary xylem) were calculated. Vessel arrangement (Fig. 1b) was described by the vessel grouping index, mean group size of grouped cells, solitary vessel tangential diameter and grouped vessel tangential diameter (von Arx and Dietz 2005; von Arx et al. 2013).

As investments into tissues might be reflected in the fibres as well (Fig. 1b), the fibre cell wall thickness and lumen diameter in the secondary xylem were measured. Three areas in distinct regions of the root cross-sections were selected for photographing under 400 × magnification with differential interference technique using Zeiss AxioImagerZ2 microscope. Only completely lignified portions of roots were selected for measurements. In each photograph, 10–15 cells were randomly selected for measurement of cell wall thickness and lumen diameter using the ZEN 2012 software.

Statistics

The effects of N, P and O_3 levels on anatomical vessel traits were tested using the R software package (R Core Team, 2017). For continuous response variables, linear mixed effects models (lme) provided in the nlme package were used, on which ANOVA Type III was applied. Factors O_3, N, P and their interactions were set as fixed effects. Taking the split plot design (Paoletti et al. 2017) into account, blocks and O_3 levels nested within the blocks were included as random effects. Model fits were assessed using visual diagnostics plots. In cases where homoscedasticity was violated, weights were added to the factor and where variance inequality was present a log transformation was used. Significant differences among groups were obtained with user-defined contrasts using general linear hypothesis testing (*glht*) provided in the multcomp package; by this way, the differences among levels of a specific variable were tested over all levels of the other variables. Where ANOVA Type III showed statistically significant effect of a selected factor, but multiple comparisons did not show significant differences among groups, Tukey's test in *glht* function was applied. Tukey's test in *glht* function seeks differences among groups without taking variation within the other main effects into account (i.e. comparing effects only at control levels of factors). For ordinal variables (number of protoxylem poles and distinctiveness of growth rings), Kruskal–Wallis tests were used to compare between P, N and O_3 levels. Correlations between vessel density and mean tangential vessel diameters were investigated using Pearson's product-moment correlation test in R.

Results

Allover, the secondary xylem of investigated 2-mm poplar roots was diffuse-porous, with 28.8 ± 0.82% being solitary vessels and a mean group size of 2.97 ± 0.03 for grouped vessels. Xylem rays were uniseriate to occasionally biseriate. Vessels were accompanied by scanty paratracheal parenchyma. As roots were less than 1 year old, emerging from cuttings in spring, the density changes inside growth rings that occurred in some roots were defined as IADFs. IADFs were either completely discernible, discernible in one part of the root or only slightly discernible. In the phloem and pericycle, tangentially arranged groups of fibre cells were observed, with cell lumina decreasing due to increasing cell wall thickness from cambium towards the outer perimeter of the root. Primary xylem was evident in the majority of investigated roots, but its shape varied from diarch, triarch, tetrarch to pentarch.

Effects of the treatments were mainly observed on tissue widths and tissue ratios, fibre anatomy and vessel grouping, while the vessel size and consequently their hydraulic properties were not affected.

Tissue widths and tissue ratios

The area of primary xylem was significantly affected by $O_3 \times N$ showing higher area of primary xylem under elevated O_3 at N0 compared to ambient O_3 at N0 (Table 1, Table S3, Fig. 2). The shape of primary xylem (i.e. the number of protoxylem poles) was affected by O_3 ($H = 7.81$, $P = 0.0052$, Fig. 3a) and phosphorus ($H = 9.87$, $P = 0.0072$, Fig. 3c), but not by N ($H = 2.36$, $P = 0.1248$, Fig. 3b). At increased O_3 levels, the number of protoxylem poles was significantly higher when compared to the control ($Z = 2.63$, $P = 0.0086$, Fig. 3a). The number of protoxylem poles was

Table 1 Results of ANOVA III type for tissue widths and tissue ratios in 2-mm roots of poplar cuttings under different combinations of O_3, N and P

	Width of periderm		Width of bark		Area of sec. xylem		Area of primary xylem		Periderm to bark ratio		Bark to sec. xylem ratio	
	χ^2	*P*	χ^2	*P*	χ^2	*P*	χ^2	*P*	χ^2	*P*	χ^2	*P*
O_3	1.30	n.s	0.18	n.s	14.96	***	3.08	"	1.10	n.s	2.75	"
P	7.34	*	4.02	n.s	7.50	*	0.83	n.s	10.28	**	3.21	n.s
N	4.31	*	0.47	n.s	0.02	n.s	0.04	n.s	2.70	n.s	0.37	n.s
$O_3 \times P$	3.07	n.s	4.47	n.s	7.23	*	0.23	n.s	0.81	n.s	0.35	n.s
$O_3 \times N$	0.08	n.s	0.60	n.s	1.60	n.s	4.45	*	0.71	n.s	0.68	n.s
$N \times P$	2.10	n.s	0.37	n.s	6.22	*	1.15	n.s	0.83	n.s	1.00	n.s
$O_3 \times N \times P$	1.00	n.s	0.18	n.s	1.75	n.s	3.73	n.s	0.45	n.s	0.34	n.s

P values are marked by *** (< 0.001), ** (< 0.01), * (< 0.05), "(< 0.1), n.s. (non-significant, ≥ 0.1)

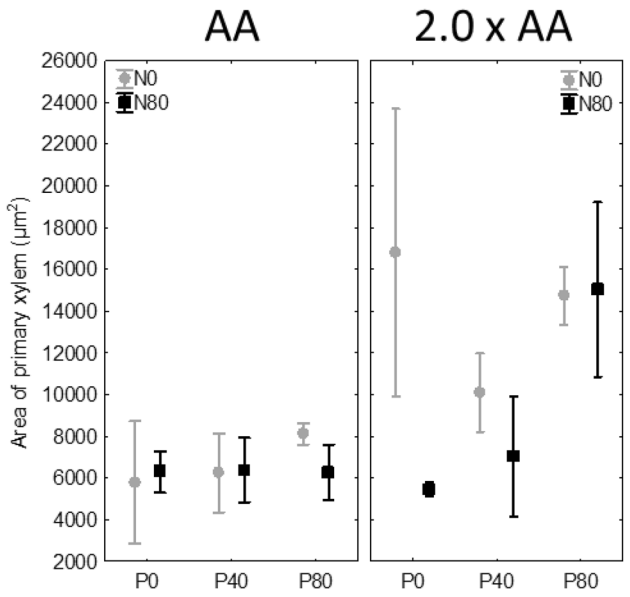

Fig. 2 Area of primary xylem (mean ± stderr.) in roots of O_3-sensitive poplar clone subjected to two levels of O_3 (AA—ambient, 2.0 × AA), two levels of N (0 and 80 kg ha^{-1}, referred as N0 and N80, respectively) and three levels of P (0, 40 and 80 kg ha^{-1}, referred as P0, P40 and P80, respectively). $N = 3$ plants per treatment combination

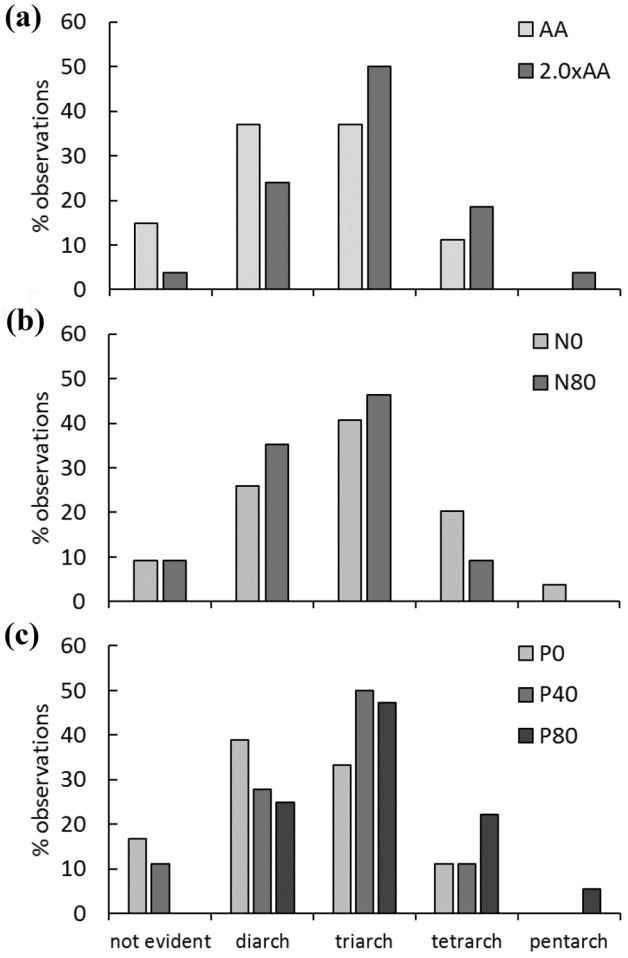

Fig. 3 Histograms for the percentage of roots with a distinct shape of the primary xylem (number of protoxylem poles) in O_3-sensitive poplar clone after exposure to two levels of O_3 (AA—ambient, 2.0 × AA), two levels of N (0 and 80 kg ha^{-1}) and three levels of P (0, 40 and 80 kg ha^{-1}). **a** Effect of O_3, **b** effect of N, **c** effect of P. From each plant, three 2-mm-thick roots were investigated ($N = 108$). When the primary xylem was not distinct it was marked as "Not evident" in the graph

also significantly higher in plants grown in P80 soil when compared to plants grown in P0 soil ($Z = 2.92$, $P = 0.0105$, Fig. 3c).

The area of the secondary xylem was affected by O_3, P and interactions of $O_3 \times P$ and $N \times P$ (Table 1, Table S3, Fig. 4a). Multiple comparisons showed a significantly higher area of the secondary xylem under elevated O_3 combined with P0 when compared to ambient O_3 combined with P0 (Fig. 4a). There was an insignificant trend for increasing secondary xylem area at ambient O_3 with increasing P concentrations while the opposite was noticed at elevated O_3. At N80 in combination with P40, the area of the secondary

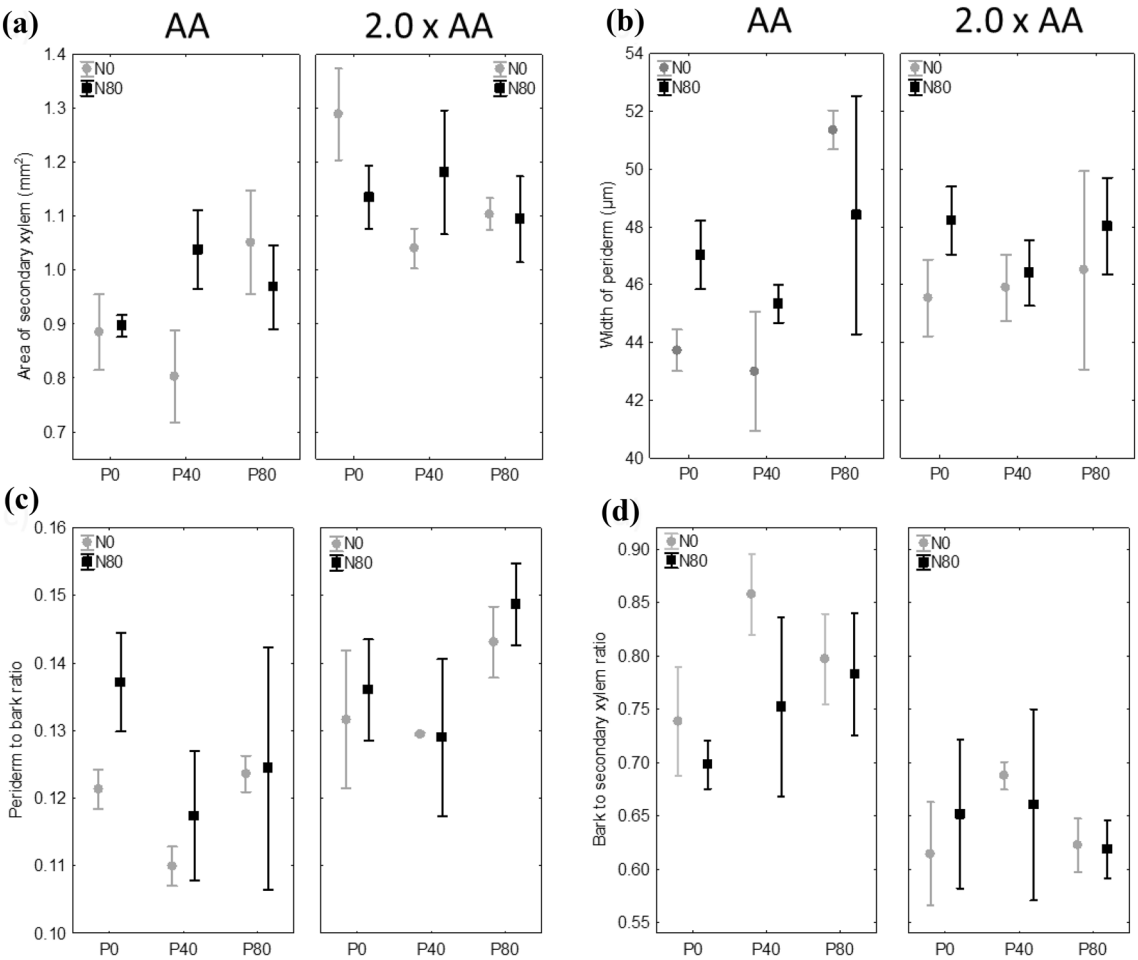

Fig. 4 Tissue widths and ratios (mean ± stderr.) in the roots of O_3-sensitive poplar clones subjected to two levels of O_3 (AA—ambient, 2.0 × AA), two levels of N (0 and 80 kg ha^{-1}, referred as N0 and N80, respectively) and three levels of P (0, 40 and 80 kg ha^{-1}, referred as P0, P40 and P80, respectively). **a** Area of the secondary xylem, **b** width of the periderm, **c** periderm to bark ratio, and **d** bark to secondary xylem ratio. $N = 3$ plants per treatment combination

xylem was significantly higher when compared to N0 in combination with P40 (Fig. 4a).

There was no effect of any parameter observed on the width of bark. The width of the periderm was significantly affected by the amount of added P and N (Table 1, Table S3, Fig. 4b). Tukey's test revealed significant wider periderm at N80 compared to N0 (Fig. 4b), while the periderm under the P80 treatment was significantly wider compared to P0 and P40 treatments (Fig. 4b).

The periderm to bark ratio was significantly affected by P. Tukey's test indicated a higher periderm to bark ratio in P80 compared to the P40 treatment (Table 1, Table S3, Fig. 4c). The bark to secondary xylem ratio showed a negative tendency with increasing O_3 (Table 1, Table S3, Fig. 4d). IADF distinctiveness was not significantly affected by any of the tested parameters (data not shown).

Cells of secondary xylem

No effect of any parameter was observed on the mean vessel tangential diameter and the cumulative area of vessels (Table 2, Table S4). Vessel density was affected by O_3, and Tukey's test has shown a significantly lower vessel density at elevated O_3 (Table 2, Fig. 5a). The percentage of conductive tissue within the xylem, and K_h (accumulated potential hydraulic conductivity) were affected by O_3 as well (Table 2, Fig. 5b, c). Tukey's test showed a higher percentage of conductive area within the xylem at control O_3 levels compared to elevated O_3 levels. The opposite effect was seen for K_h. No effect was shown for xylem-specific potential hydraulic conductivity (Table 2, Table S4).

The correlation between tangential vessel diameter and vessel density was higher under ambient O_3 than under

Table 2 Results of ANOVA III type for secondary xylem cell dimensions in 2-mm roots of poplar cuttings under different combinations of O_3, N and P. K_h: accumulated potential hydraulic conductivity

	Vessel density		Cumulative area of vessels		Conductive area within xylem		K_h	
	χ^2	*P*	χ^2	*P*	χ^2	*P*	χ^2	*P*
O_3	12.9	***	0.96	n.s	4.99	*	37.1	****
P	2.63	n.s	1.75	n.s	3.48	n.s	4.66	"
N	0.60	n.s	1.50	n.s	1.14	n.s	1.61	n.s
O_3×P	3.92	n.s	0.86	n.s	1.50	n.s	0.82	n.s
O_3×N	2.70	n.s	0.04	n.s	0.28	n.s	0.04	n.s
N×P	3.10	n.s	1.78	n.s	1.63	n.s	1.62	n.s
O_3×N×P	1.65	n.s	0.65	n.s	0.01	n.s	0.37	n.s
	Xylem-specific potential hydraulic conductivity		Vessel grouping index		Mean group size of grouped cells		Mean tangential vessel lumen diameter	
	χ^2	*P*	χ^2	*P*	χ^2	*P*	χ^2	*P*
O_3	2.09	n.s	6.84	**	10.2	**	1.09	n.s
P	3.67	n.s	7.18	*	8.37	**	4.49	n.s
N	1.51	n.s	7.07	**	7.46	*	1.42	n.s
O_3×P	0.40	n.s	5.42	"	11.7	***	0.98	n.s
O_3×N	0.01	n.s	6.53	*	4.15	n.s	0.14	n.s
N×P	1.47	n.s	13.95	***	12.7	**	1.51	n.s
O_3×N×P	0.03	n.s	10.99	**	10.6	**	1.03	n.s
	Mean solitary vessel tangential cell lumen diameter		Mean group vessel tangential cell lumen diameter		Fibre cell wall thickness		Fibre cell lumen radial diameter	
	χ^2	*P*	χ^2	*P*	χ^2	*P*	χ^2	*P*
O_3	0.08	n.s	0.03	n.s	2.44	n.s	1.28	n.s
P	2.38	n.s	0.98	n.s	3.61	n.s	1.95	n.s
N	1.40	n.s	1.14	n.s	4.46	*	0.90	n.s
O_3×P	0.58	n.s	0.21	n.s	2.51	n.s	2.60	n.s
O_3×N	0.20	n.s	0.02	n.s	6.78	**	0.00	n.s
N×P	0.97	n.s	0.96	n.s	1.83	n.s	9.72	**
O_3×N×P	0.47	n.s	0.73	n.s	2.69	n.s	2.65	n.s

K_h: accumulated potential hydraulic conductivity

P values are marked with ****(< 0.0001), ***(< 0.001), **(< 0.01), *(< 0.05), "(< 0.1), n.s. (non-significant, ≥ 0.1)

elevated O_3 (Table 3, Fig. 6). Small vessels occurred with higher density under ambient O_3 compared to elevated O_3 and vice versa for large vessels (Fig. 6). In the case of nutrients, higher correlation coefficients for vessel density and vessel tangential diameter were found for higher addition of nutrients (Table 3, Fig. 6).

The vessel grouping index was responsive to single factors O_3, N and P and their tripartite interaction (Table 2, Fig. 7). The effect of nutrients was only significant at ambient O_3. At P0 combined with ambient O_3, vessel grouping index in roots with no added N was significantly higher compared to treatment with added N or elevated O_3. At the intermediate phosphorus level (P40), there was no significant effect of O_3 or N addition, while at high P (P80), the vessel grouping index was higher at ambient O_3 with N80 addition.

The mean group size of grouped vessels was influenced by O_3, P, N and O_3×P, N×P and O_3×N×P interactions (Table 2, Fig. S1). Overall, a smaller number of vessels occurred in groups under elevated O_3. However, the response to O_3 was modulated by the presence of N and P in the same way as the vessel grouping index—groups of vessels contained higher number of vessels under N0–P0 and N80–P80, both under ambient O_3 (Table 2, Fig. S1). When separate diameter measurements of solitary and grouped vessels were performed, no effect of any investigated parameter was detected (Table 2, Table S4).

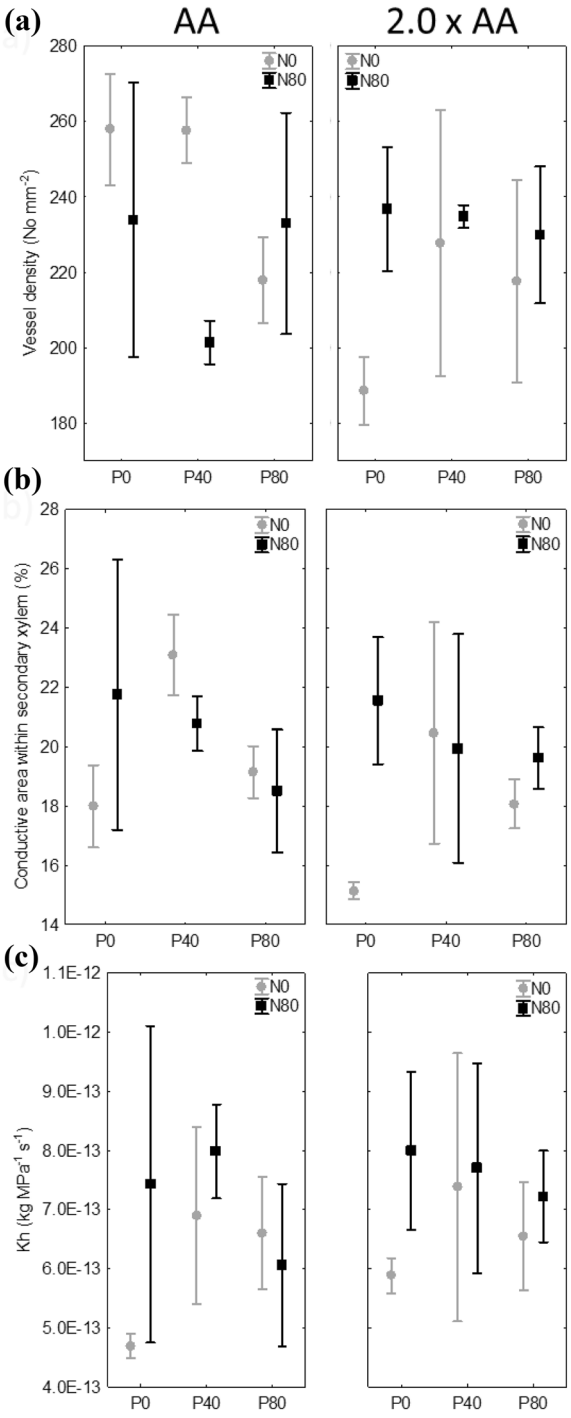

Fig. 5 **a** Vessel density, **b** conductive area within the secondary xylem, and **c** accumulated potential hydraulic conductivity—K_h (mean ± stderr.) in the roots of O_3-sensitive poplar clone subjected to two levels of O_3 (AA—ambient, 2.0 × AA), two levels of N (0 and 80 kg ha^{-1}, referred as N0 and N80, respectively) and three levels of P (0, 40 and 80 kg ha^{-1}, referred as P0, P40 and P80, respectively). $N = 3$ plants per treatment combination

Table 3 Pearson's correlation coefficients (R) between tangential vessel diameter and vessel density in roots of poplar clone grown under two levels of O_3 (AA—ambient, 2.0 × AA), N (0 and 80 kg ha^{-1}, referred as N0 and N80, respectively) and three levels of P (0, 40 and 80 kg ha^{-1}, referred as P0, P40 and P80, respectively)

Factor	Factor level	R	P
O_3	AA	− 0.83	< 0.0001****
	2.0 × AA	− 0.54	0.0021**
N	N0	− 0.53	0.0250*
	N80	− 0.85	< 0.0001****
P	P0	− 0.62	0.0310*
	P40	− 0.69	0.0131*
	P80	− 0.85	0.0004***

P values are marked with ****(< 0.0001), ***(< 0.001), **(< 0.01), *(< 0.05)

The cell wall thickness of fibres was affected by N, and O_3 × N interaction. At elevated O_3, the addition of N did not change cell wall thickness, while at ambient O_3, the addition of N resulted in significantly thicker cell wall (Table 2, Fig. 8a). The cell lumen of fibres was affected by N × P interaction (Table 2). When N was added to the P40 treatment, the cell lumen was significantly smaller when compared to the P40 treatment with no added N. At P0 and P80, there was no effect of N addition on the cell lumen (Table 2, Fig. 8b).

Discussion

Width and shape of tissues and tissue ratios

The responses of tissues within thin transport roots of O_3-sensitive poplar clone to elevated O_3 and different nutrient levels were very specific. Therefore, our hypothesis that elevated O_3 will negatively affect root tissue widths and that the effect will be more pronounced at higher nutrient levels was not confirmed. Starting from the primary xylem, elevated O_3 and increasing P concentrations positively affected the number of protoxylem poles. O_3 acted in interaction with N on the area of primary xylem and in interaction with P on the area of secondary xylem. In both cases, there was a significant positive response to elevated O_3 within treatments with no added N or P, respectively. On the other hand, O_3 had no effect on widths of periderm and bark under any nutrient treatments.

The number of protoxylem poles affects the morphology of the root system as lateral roots emerge from the sites adjacent to the protoxylem poles (Fayle 1975). Root

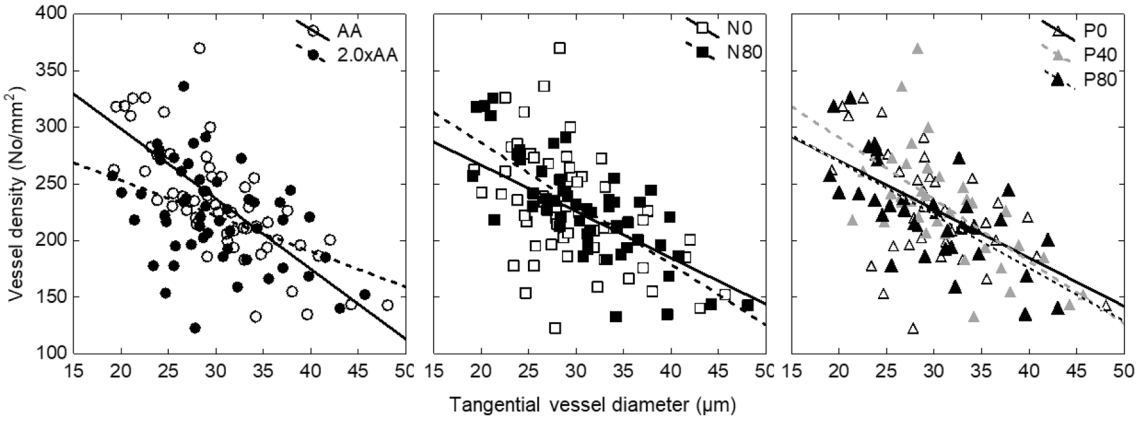

Fig. 6 Effects of O_3 (AA—ambient, 2.0 × AA), N (0 and 80 kg ha^{-1}, referred as N0 and N80, respectively) and P (0, 40 and 80 kg ha^{-1}, referred as P0, P40 and P80, respectively) on the correlation between vessel tangential diameter and vessel density

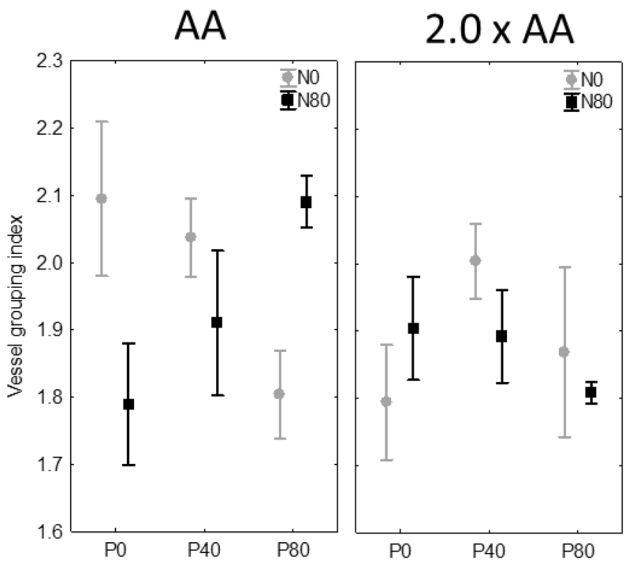

Fig. 7 Interactive effects of O_3, N and P on the vessel grouping index (mean ± stderr.) in O_3-sensitive poplar clone subjected to two levels of O_3 (AA—ambient, 2.0 × AA), two levels of N (0 and 80 kg ha^{-1}, referred as N0 and N80, respectively) and three levels of P (0, 40 and 80 kg ha^{-1}, referred as P0, P40 and P80, respectively). $N = 3$ plants per treatment combination

vasculature pattern is regulated by mutually inhibitory interactions between auxin and cytokinin, where primary xylem development is promoted by auxin (Bishopp et al. 2011). Exposure to elevated O_3 has been reported to change tree hormonal status of ethylene, abscisic acid to auxin ratio and cytokinins (Kraigher et al. 2008; Hoshika et al. 2019; Podda et al. 2019). As plant development under stress conditions is regulated by the interplay of different hormonal pathways (O'Brien and Benková 2013), elevated O_3 may have a modulatory effect on the development of tissues. P is also a known strong modulator of root architecture (Niu et al. 2013). However, the morphological response of the fine root systems (< 2 mm) from the same experiment did not reveal any effect of P or O_3 on root branching density (Mrak et al. 2020). As P was not the main limiting nutrient for biomass growth in any of the concentration applied in this experiment (Zhang et al. 2018; Mrak et al. 2020), it appears that an anatomical predisposition for higher number of lateral roots did not manifest in the actual lateral root formation.

The diameter of the primary xylem was found to be closely correlated to the number of the protoxylem poles (Horsley and Wilson 1971), which was confirmed in our study (data not shown). Furthermore, the number of protoxylem poles is positively associated with the longevity of roots, i.e. triarch and tetrarch roots tend to form secondary roots, whereas diarch roots tend to die before transition into secondary growth (Hishi and Takeda 2005a, b). Production or initiation of roots with potentially greater longevity would be beneficial for a tree as it would reduce the costs for production of new roots under the O_3 exposure which is known to reduce the supply of carbohydrates belowground (Andersen 2003).

An increased area of secondary xylem due to elevated O_3 was reflected in the lower bark to secondary xylem ratio under elevated O_3. The lower bark to secondary xylem ratio indicates a greater investment into xylem and less into phloem. This is the opposite to what was found for oak roots under elevated O_3 in well-watered conditions (Mrak et al. 2019). However, the greater secondary xylem area in poplar roots under elevated O_3 was not reflected in the root biomass of the same plants, as root biomass under elevated O_3 was decreased (Mrak et al. 2020), indicating a changed structure of the secondary xylem and bark that could manifest as decreased cell wall thickness or changes in chemical structure. Greater secondary xylem area was also not reflected in the cumulative area of vessels, but it was reflected in the increased accumulated potential hydraulic conductivity

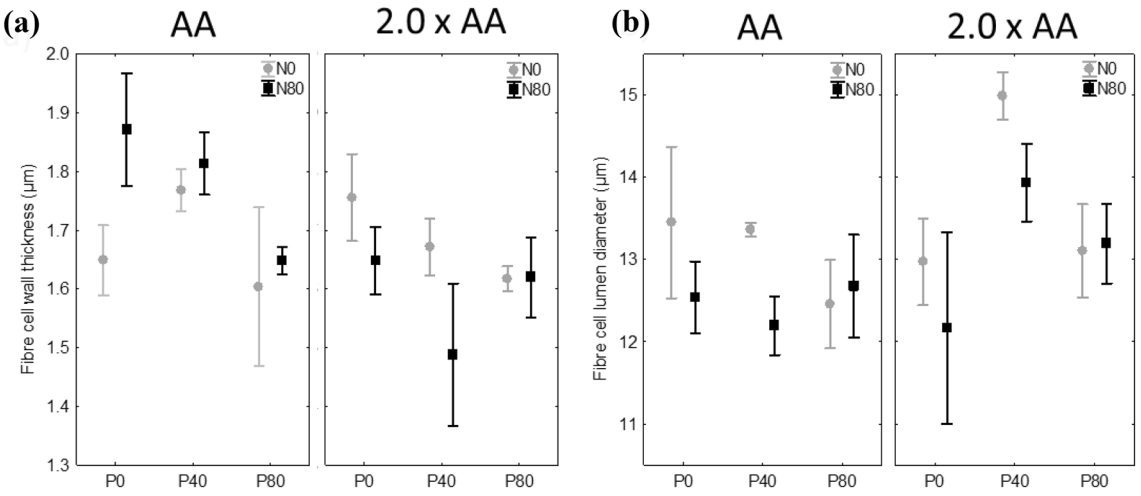

Fig. 8 Fibre cell wall thickness (**a**) and fibre cell lumen diameter (**b**) (mean ± stderr.) in the secondary xylem of O_3-sensitive poplar clone roots subjected to two levels of O_3 (AA—ambient, 2.0 x AA), two levels of N (0 and 80 kg ha^{-1}, referred as N0 and N80, respectively) and three levels of P (0, 40 and 80 kg ha^{-1}, referred as P0, P40 and P80, respectively). (Mean ± stderr.), $N = 3$ plants per treatment combination

(K_h) which could supply greater amounts of water to the aboveground parts. As O_3 induces stomatal sluggishness and increases night-time stomatal conductance in this poplar clone, water use efficiency of the O_3-stressed trees is reduced and might be compensated by greater delivery of water to the aboveground parts (Hoshika et al. 2015, 2019). Changes in auxin concentration were found to control the expression of genes in the process of secondary xylem formation, but ethylene and gibberellin appear to be involved, too (Nilsson et al. 2008). The application of ethylene to hybrid poplar stems induced 5 × thicker xylem and 2 × thicker phloem formation (Junghans et al. 2004). O_3 treatment is usually associated with a decrease in secondary xylem width (Matyssek et al. 2002; Kaakinen et al. 2004), while our contradictory results correspond to results of Makkonen et al. (2016) who found increased widths of growth rings under O_3 exposure in spruce. As ethylene was shown to increase in leaves of O_3 treated trees (*Q. ilex*; Cotrozzi et al. 2017, poplar Oxford clone; Hoshika et al. 2019), it might be possible that it exerts effects on root anatomogenesis due to its freely diffusable nature (Park et al. 2017).

Cells of secondary xylem

Contrary to our expectations elevated O_3 did not exert a negative effect on vessel sizes, which were also not affected by nutrient addition. However, elevated O_3 decreased vessel density and acted in a tripartite interaction with N and P on the vessel grouping pattern. The negative effect of elevated O_3 was confirmed for cell wall thickness of secondary xylem fibres where O_3 acted in interaction with N, while the fibre lumen was affected only by N × P interaction.

Generally, vessel density and vessel size in plants are regulated with decreasing auxin levels from shoots to roots. Therefore, lower levels of auxin in roots result in a lower density and bigger size of vessels in roots (Aloni 2007). It was shown that O_3 has a modulating effect on auxin polar transport and stimulates stress-induced morphogenic responses in *Arabidopsis* (Blomster et al. 2011), while elevated O_3 was reported to decrease an expression of auxin-binding protein (ABP1) in leaves of moderately O_3 tolerant *Populus tremuloides* clone (Gupta et al. 2005). However, the role of ABP1 in auxin perception and signalling is still unclear (Gelová et al. 2021). Based on these two reports, the effects of elevated O_3 on vessel density via auxin cannot be excluded. In our experiment, the vessel density in roots was negatively affected by O_3, but interestingly no effect on vessel size was observed. It appears that vessel density is a more sensitive parameter than vessel size, corresponding to findings of Schume et al. (2004). In an experiment containing three species of oak, across all three species the response to O_3 was an increased vessel density, while a decrease in vessel size was observed only in one of the investigated species (Mrak et al. 2019). Although the plants from our experiment had a significantly higher total biomass when supplied with additional N (+97%, Zhang et al. 2018), this increased growth was not reflected in increased potential hydraulic conductivity (K_s, directly correlated to vessel size and density, and K_h, directly correlated to vessel size and number) as theoretically proposed by Goldstein et al. (2013) and supported by several studies. The fast growth might not be related to any specific anatomical feature of branch or coarse root xylem, but merely to empirical (i.e. measured) sapwood area-specific hydraulic conductivity (K_s) (Hajek et al. 2014).

The absence of the correlation between the growth rate and vessel size has been explained by the properties of the vessel pit membrane structure (Hajek et al. 2014). In our experiment, the absence of any specific effect of O_3 and nutrients on vessel size or xylem-specific potential conductivity could also be result of very high variability in vessel size inside the roots of a single plant (Fig. S2). As pointed out by Hajek et al. (2014), roots have a considerable anatomical plasticity reflecting their functional diversity, which means that within a given diameter class significantly different potential xylem-specific hydraulic conductivity can be encountered due to the presence of high conductivity roots.

As mentioned above, vessel density but not vessel size was affected by O_3 despite their previously reported tight correlation (Schume et al. 2004, Savage et al. 2010). Our results revealed that a stronger correlation between tangential vessel diameter and vessel density was encountered under ambient O_3, indicating a slight dysregulation of vessel formation under elevated O_3. Therefore, small vessels occurred with higher density under ambient O_3 compared to elevated O_3. In the case of nutrients, stronger correlations between vessel density and vessel tangential diameter were found for higher addition of nutrients.

The pattern of vessel grouping within a single species is associated with exposure to stress (Zhao 2016) and fertilisation (Spannl et al. 2016). Within species there is a positive correlation between vessel grouping and habitat dryness (Carlquist 1966; von Arx et al. 2013; Schuldt et al. 2016). It was suggested that vessel grouping may result in higher likelihood of cavitation advancement through the neighbouring vessels (von Arx et al. 2013 and references therein), or alternatively greater resistance to cavitation (Schuldt et al. 2016). In relation to nutrient addition, fertilisation with N and N + P resulted in an increased vessel grouping index and a higher mean vessel group size in the stem of tropical montane tree species (Spannl et al. 2016). In our experiment, the vessel grouping index and mean vessel group size were highest in combination of N0–P0 with AA, and N80–P80 with AA, indicating that only balanced N:P ratios induce vessel grouping. Elevated O_3 obviously prevented the modulating effect of nutrients on the vessel grouping index. It has been reported that inhibition of polar auxin transport in hybrid poplars induces clustering of vessels (Junghans et al. 2004; Johnson et al. 2018). Based on this finding, we suggest that during xylogenesis under specific nutrient combinations in ambient O_3, decreased auxin transport in roots is encountered. In the light of functionality of the water conducting system, elevated O_3 prevents the adaptation of cavitation resistance to changing ratios of N and P.

Our finding that at ambient O_3 the addition of N significantly increased fibre cell wall thickness in the secondary xylem, while at elevated O_3 levels addition of N had no effect on cell wall thickness may indicate that elevated O_3 reduced carbon allocation for cell wall formation. This is in accordance with the finding that cellulose synthesis in poplars is reduced under elevated O_3 (Richet et al. 2011). The reduction of the cellulose to lignin ratio could be a compensatory mechanism that would allow radial growth with lower carbon costs. The fact that elevated O_3 prevented the use of N for fibre cell wall synthesis is also in concert with the results revealed in our previous paper detailing that the biomass of roots from O_3 treated plants is lower (Mrak et al. 2020) and that plants exposed to elevated O_3 cannot fully exploit available N in soil due to a smaller root surface area per soil volume (Mrak et al. 2020).

Radial expansion of fibres is controlled by auxin as well (Nilsson et al. 2008). In our study, the cell lumen of fibres was affected by N × P interaction. When N was added to P40 treatment, the cell lumen was significantly larger than when compared to treatments with no added N, while at P0 and P80, no effect was observed. These results indicate the importance of nutrient ratios on root anatomical responses, as already indicated by the vessel grouping pattern.

Conclusions

The results of our study indicate that poplar root anatomical properties were changed by the elevated O_3. Responses depended on the tissue or cell type and were mainly affected by the N and/or P levels. Our results suggest that under elevated O_3, compensatory mechanisms are switched on, that may change tree functioning. In conditions of elevated O_3, the increased secondary xylem area resulted in increased accumulated potential hydraulic conductivity (K_h) that could compensate for O_3-induced decreased water use efficiency. Elevated O_3 could prevent the adaptation of cavitation resistance to changing ratios of nutrients through its effect on vessel grouping, which could potentially affect the survival of trees under drought or frost. Most importantly, the application of N in combination with elevated O_3 did not result in an increased fibre cell thickness as it happened under ambient O_3, indicating C-saving mechanisms. Wood under elevated O_3 would be less dense, with implications for C sequestration belowground and strength of root anchoring into the soil. Several responses related to auxin found in this study point to importance of elucidation of nutrient ratios and O_3 effects on trees from the perspective of plant hormones. As our current study mainly focused on anatomical structure of roots in the terms of function in transport of water and solutes, it would be necessary to investigate the role of roots as storage organs (i.e. the amount of parenchyma cells in primary and secondary tissues) under O_3 exposure combined with different nutrient levels or ratios in the future.

Author contribution statement

EP and HK: funding acquisition (Italian and Slovenian part, respectively), YH and EP: experiment conceptualization; JG and TM: methodology and data collection; ND and TM: data analysis; and TM: original draft preparation. All the authors—writing review and editing.

Supplementary Information The online version contains supplementary material available at https://doi.org/10.1007/s00468-021-02111-0.

Acknowledgements We would like to thank Melita Hrenko from the Department of Tree Physiology and Genetics of Slovenian Forestry Institute and students from Biotechnical Centre Naklo, Slovenia, for cleaning of poplar roots, while Gregor Skoberne from Department of Forest Yield and Silviculture is acknowledged for preparation of root cross-sections. Moreno Lazzara, Alessandro Materassi and Gianni Fasano are greatly acknowledged for support during field work with the O_3 FACE. Philip Brailey-Jones is acknowledged for English language editing.

Funding The study was funded by Slovenian Research Agency Research Programme P4-0107, LIFEGENMON (LIFE ENV/SI/000148) co-financed by the European LIFE financial programme, the national ministries in Slovenia, Germany and Greece and all project beneficiaries, the Fondazione Cassa di Risparmio di Firenze (2013/7956) and the LIFE15 ENV/IT/000183 project MOTTLES.

Data availability The authors confirm that the data supporting the findings of this study are available within the article and its supplementary materials.

Declarations

Conflict of interest The authors declare no conflict of interest.

Consent for publication All the authors have read and agreed to the published version of the manuscript.

References

Aloni R (2007) Phytohormonal mechanisms that control wood quality formation in young and mature trees. In: Entwistle K, Harris P, Walker J (eds) The compromised wood workshop 2007. The Wood Technology Research Centre University of Canterbury, Christchurch, pp 1–22

Andersen CP (2003) Source–sink balance and carbon allocation below ground in plants exposed to ozone. New Phytol 157:213–228

Arevalo CBM, Bhatti JS, Chang SX, Sidders D (2011) Land use change effects on ecosystem carbon balance: from agricultural to hybrid poplar plantation. Agric Ecosyst Environ 141:342–349

Bishopp A, Help H, El-Showk S, Weijers D, Scheres B, Friml J, Benková E, Mähönen AP, Helariutta Y (2011) A mutually inhibitory interaction between auxin and cytokinin specifies vascular pattern in roots. Curr Biol 21:917–926

Blomster T, Salojärvi J, Sipari N, Brosché M, Ahlfors R, Keinänen M, Overmyer K, Kangasjärvi J (2011) Apoplastic reactive oxygen species transiently decrease auxin signaling and cause stress-induced morphogenic response in Arabidopsis. Plant Physiol 157:1866–1883

Carlquist S (1966) Wood anatomy of Compositae: a summary, with comments on factors controlling wood evolution. Aliso 6:25–44

Cotrozzi L, Pellegrini E, Guidi L, Landi M, Lorenzini G, Massai R, Remorini D, Tonelli M, Trivellini A, Vernieri P, Nali C (2017) Losing the warning signal: drought compromises the cross-talk of signaling molecules in *Quercus ilex* exposed to ozone. Front Plant Sci 8:1020

De Micco V, Campelo F, De Luis M, Bräuning A, Grabner M, Battipaglia G, Cherubini P (2016) Intra-annual density fluctuations in tree rings: how, when, where and why? IAWA J 37:232–259

Fayle DCF (1975) Archy and diameter of primary xylem in horizontal and vertical roots of red pine. Can J For Res 5:122–129

Fenn ME, Baron JS, Allen EB, Rueth HM, Nydick KR, Geiser L, Bowman WD, Sickman JO, Meixner T, Johnson DW, Neitlich P (2003) Ecological effects of nitrogen deposition in the western United States. Bioscience 53:391–403

Gelová Z, Gallei M, Pernisová M, Brunoud G, Zhang X, Glanc M, Li L, Michalko J, Pavlovičová Z, Verstraeten I, Han H, Hajný J, Hauschild R, Čovanová M, Zwiewka M, Hoermayer L, Fendrych M, Xu T, Vernoux T, Friml J (2021) Developmental roles of Auxin Binding Protein 1 in *Arabidopsis thaliana*. Plant Sci 303:110750

Goldstein G, Bucci SJ, Scholz FG (2013) Why do trees adjust water relations and hydraulic architecture in response to nutrient availability? Tree Physiol 33:238–240

Gupta P, Duplessis S, White H, Karnosky DF, Martin F, Podila GK (2005) Gene expression patterns of trembling aspen trees following long-term exposure to interacting elevated CO_2 and tropospheric O_3. New Phytol 167:129–142

Hajek P, Leuschner C, Hertel D, Delzon S, Schuldt B (2014) Trade-offs between xylem hydraulic properties, wood anatomy and yield in *Populus*. Tree Physiol 34:744–756

Hishi T, Takeda H (2005a) Dynamics of heterorhizic root systems: protoxylem groups within the fine-root system of *Chamaecyparis obtusa*. New Phytol 167:509–521

Hishi T, Takeda H (2005b) Life cycles of individual roots in fine root system of *Chamaecyparis obtusa* Sieb. et Zucc. J For Res 10:181–187

Hoosbeek MR, Lukac M, van Dam D, Godbold DL, Velthorst EJ, Biondi FA, Peressotti A, Cortufo MF, de Angelis P, Scarascia-Mugnozza G (2004) More new carbon in the mineral soil of a poplar plantation under Free Air Carbon Enrichment (POPFACE): cause of increased priming effect? Global Biogeochem Cycles 18

Horsley SB, Wilson BF (1971) Development of the woody portion of the root system of *Betula papyrifera*. Am J Bot 58:141–147

Hoshika Y, Katata G, Deushi M, Watanabe M, Koike T, Paoletti E (2015) Ozone-induced stomatal sluggishness changes carbon and water balance of temperate deciduous forests. Sci Rep 5:09871

Hoshika Y, Carrari E, Zhang L, Carriero G, Pignatelli S, Fasano G, Materassi A, Paoletti E (2018) Testing a ratio of photosynthesis to O_3 uptake as an index for assessing O_3-induced foliar visible injury in poplar trees. Environ Sci Pollut Res 25:8113–8124

Hoshika Y, De Carlo A, Baraldi R, Neri L, Carrari E, Agathokleous E, Zhang L, Fares S, Paoletti E (2019) Ozone-induced impairment of night-time stomatal closure in O_3-sensitive poplar clone is affected by nitrogen but not by phosphorus enrichment. Sci Tot Environ 692:713–722

Isebrands JG, Richardson J (2014) Poplars and willows: trees for society and the environment. CAB International and FAO, Rome

Johnson D, Eckart P, Alsamadisi N, Noble H, Martin C, Spicer R (2018) Polar auxin transport is implicated in vessel differentiation and spatial patterning during secondary growth in *Populus*. Am J Bot 105:186–196

Junghans U, Langenfeld-Heyser R, Polle A, Teichmann T (2004) Effect of auxin transport inhibitors and ethylene on the wood anatomy of poplar. Plant Biol (Stuttg) 7:22–29

Kaakinen S, Kostiainen K, Ek F, Saranpää P, Kubiske ME, Sober J, Karnosky DF, Vapaavuori E (2004) Stem wood properties of

Populus tremuloides, *Betula papyrifera* and *Acer saccharum* saplings after 3 years of treatments to elevated carbon dioxide and ozone. Glob Chang Biol 10:1513–1525

Kraigher H, Grebenc T, Hanke DE (2008) Ozone stress and ectomycorrhizal root–shoot signaling. In: Varma A (ed) Mycorrhiza: state of the art, genetics and molecular biology, eco-function, biotechnology, ecophysiology, structure and systematics. Springer, Berlin, pp 337–357

Lewandowski I, Bahrs E, Dahmen N, Hirth T, Rausch T, Weidtmann A (2019) Biobased value chains for a growing bioeconomy. GCB Bioenergy 11:4–8

Lewis JD, Strain BR (1996) The role of mycorrhizas in the response of *Pinus taeda* seedlings to elevated CO_2. New Phytol 133:431–443

Makkonen S, Huuhilo K, Utriainen J, Holopainen T, Kainulainen P (2016) Radial ring width and wood structure in the ozone-exposed Norway spruce seedlings grown under different nitrogen regimes. Boreal Environ Res 21:149–165

Mao Q, Watanabe M, Makoto K, Kita K, Koike T (2014) High nitrogen deposition may enhance growth of a new hybrid larch F1 growing at two phosphorus levels. Landsc Ecol Eng 10:1–8

Matyssek R, Günthardt-Goerg M, Maurer S, Christ R (2002) Tissue structure and respiration of stems of *Betula pendula* under contrasting ozone exposure and nutrition. Trees 16:375–385

Maurer S, Matyssek R (1997) Nutrition and the ozone sensitivity of birch (*Betula pendula)*. Trees 12:11–20

Monks PS, Archibald AT, Colette A, Cooper O, Coyle M, Derwent R, Fowler D, Granier C, Law KS, Mills GE, Stevenson DS, Tarasova O, Thouret V, von Schneidemesser E, Sommariva R, Wild O, Williams ML (2015) Tropospheric ozone and its precursors from the urban to the global scale from air quality to short-lived climate forcer. Atmos Chem Phys 15:8889–8973

Mrak T, Gričar J (2016) Atlas of woody plant roots. Morphology and anatomy with special emphasis on fine roots. 1st edition. The Silva Slovenica Publishing Centre, Ljubljana

Mrak T, Štraus I, Grebenc T, Gričar J, Hoshika Y, Carriero G, Paoletti E, Kraigher H (2019) Different belowground responses to elevated ozone and soil water deficit in three European oak species (*Quercus ilex*, *Q. pubescens* and *Q. robur*). Sci Tot Environ 651:1310–1320

Mrak T, Eler K, Badea O, Hoshika Y, Carrari E, Paoletti E, Kraigher H (2020) Elevated ozone prevents acquisition of available nitrogen due to smaller root surface area in poplar. Plant Soil 450:585–599

Nilsson J, Karlberg A, Antti H, Lopez-Vernaza M, Mellerowicz E, Perrot-Rechenmann C, Sandberg G, Bhalerao RP (2008) Dissecting the molecular basis of the regulation of wood formation by auxin in hybrid aspen. Plant Cell 20:843–855

Niu YF, Chai RS, Jin GL, Wang H, Tang CX, Zhang YS (2013) Responses of root architecture development to low phosphorus availability: a review. Ann Bot 112:391–408

O'Brien JA, Benková E (2013) Cytokinin cross-talking during biotic and abiotic stress responses. Front Plant Sci 4:451–451

Paoletti E, Materassi A, Fasano G, Hoshika Y, Carriero G, Silaghi D, Badea O (2017) A new-generation 3D ozone FACE (Free Air Controlled Exposure). Sci Tot Environ 575:1407–1414

Park J, Lee Y, Martinoia E, Geisler M (2017) Plant hormone transporters: what we know and what we would like to know. BMC Biol 15:93–93

Pell EJ, Sinn JP, Johansen CV (1995) Nitrogen supply as a limiting factor determining the sensitivity of *Populus tremuloides* Michx. to ozone stress. New Phytol 130:437–446

Peng Y, Chen G, Chen G, Li S, Peng T, Qiu X, Luo J, Yang S, Hu T, Hu H, Xu Z, Liu L, Tang Y, Tu L (2017) Soil biochemical responses to nitrogen addition in a secondary evergreen broad-leaved forest ecosystem. Sci Rep 7:2783

Podda A, Pisuttu C, Hoshika Y, Pellegrini E, Carrari E, Lorenzini G, Nali C, Cotrozzi L, Zhang L, Baraldi R, Neri L, Paoletti E (2019) Can nutrient fertilization mitigate the effects of ozone exposure on an ozone-sensitive poplar clone? Sci Tot Environ 657:340–350

Richet N, Afif D, Huber F, Pollet B, Banvoy J, El Zein R, Lapierre C, Dizengremel P, Perré P, Cabané M (2011) Cellulose and lignin biosynthesis is altered by ozone in wood of hybrid poplar (*Populus tremula*×*alba*). J Exp Bot 62:3575–3586

Schmutz P, Bucher JB, Günthardt-Goerg MS, Tarjan D, Landolt W (1995) Response of poplar to ozone alone and in combination with NO_2 at different nitrogen fertilization levels. Phyton-Ann Rei Bot 35:269–289

Schuldt B, Knutzen F, Delzon S, Jansen S, Müller-Haubold H, Burlett R, Clough Y, Leuschner C (2016) How adaptable is the hydraulic system of European beech in the face of climate change-related precipitation reduction? New Phytol 210:443–458

Schume H, Grabner M, Eckmüllner O (2004) The influence of an altered groundwater regime on vessel properties of hybrid poplar. Trees 18:184–194

Spannl S, Homeier J, Bräuning A (2016) Nutrient-induced modifications of wood anatomical traits of *Alchornea lojaensis* (Euphorbiaceae). Front Earth Sci 4

Thomas RB, Lewis JD, Strain BR (1994) Effects of leaf nutrient status on photosynthetic capacity in loblolly pine (*Pinus taeda* L.) seedlings grown in elevated atmospheric CO2. Tree Physiol 14:947–960

Tissue DT, Lewis JD (2010) Photosynthetic responses of cottonwood seedlings grown in glacial through future atmospheric CO_2 vary with phosphorus supply. Tree Physiol 30:1361–1372

Tyree MT, Zimmermann MH (2002) Xylem structure and the ascent of sap, 2nd edn. Springer-Verlag, Berlin

Utriainen J, Holopainen T (2001) Nitrogen availability modifies the ozone responses of Scots pine seedlings exposed in an open-field system. Tree Physiol 21:1205–1213

Verstraeten WW, Neu JL, Williams JE, Bowman KW, Worden JR, Boersma KF (2015) Rapid increases in tropospheric ozone production and export from China. Nature Geosci 8:690–695

von Arx G, Carrer M (2014) ROXAS—a new tool to build centuries-long tracheid-lumen chronologies in conifers. Dendrochronologia 32:290–293

von Arx G, Dietz H (2005) Automated image analysis of annual rings in the roots of perennial forbs. Int J Plant Sci 166:723–732

von Arx G, Kueffer C, Fonti P (2013) Quantifying vessel grouping—added value from the image analysis tool ROXAS. IAWA J 34:433–445

Watanabe M, Yamaguchi M, Matsumura H, Kohno Y, Izuta T (2012) Risk assessment of ozone impact on *Fagus crenata* in Japan: consideration of atmospheric nitrogen deposition. Eur J For Res 131:475–484

Wittig VE, Ainsworth EA, Naidu SL, Karnosky DF, Long SP (2009) Quantifying the impact of current and future tropospheric ozone on tree biomass, growth, physiology and biochemistry: a quantitative meta-analysis. Glob Change Biol 15:396–424

Young PJ, Archibald AT, Bowman KW, Lamarque J-F, Naik V, Stevenson DS, Tilmes S, Voulgarakis A, Wild O, Bergmann D, Cameron-Smith P, Cionni I, Collins WJ, Dalsøren SB, Doherty RM, Eyring V, Faluvegi G, Horowitz LW, Josse B, Lee YH, MacKenzie IA, Nagashima T, Plummer DA, Righi M, Rumbold ST, Skeie RB, Shindell DT, Strode SA, Sudo K, Szopa S, Zeng G (2013) Pre-industrial to end 21st century projections of tropospheric ozone from the Atmospheric Chemistry and Climate Model Intercomparison Project (ACCMIP). Atmos Chem Phys 13:2063–2090

Zhang L, Hoshika Y, Carrari E, Badea O, Paoletti E (2018) Ozone risk assessment is affected by nutrient availability: evidence from a simulation experiment under free air controlled exposure (FACE). Environ Pollut 238:812–822

Zhao X (2016) Spatial variation of vessel grouping in the xylem of *Betula platyphylla* Roth. J Plant Res 129:29–37